

Phys 499: Final Report

Optical transport of cold atoms

MengXing Na, 1297073^{1,*}

¹Department of Physics, University of Alberta, Edmonton, AB, Canada T6G 2G7

In order to interface a cloud of ultracold rubidium atoms with a nanomechanical device, the cloud needs to be transported a macroscopic distance of approximately 30cm. To do this, we make use of focus-tunable lenses from Optotune to electronically control the focus of an infrared laser with wavelenth of 1064nm. The focus of the laser creates a red-detuned dipole trap for the atoms. The heating of the transport is modelled in the non-adiabatic regime to ensure that the cold gas cloud does not escape from the trap during transport. The current system's trap depth is on the shallow side, consequence of a waist that is slight too large. Replacing lens 1 with a smaller focal length lens should fix the problem.

I. INTRODUCTION

In the last two decades, laser cooling and trapping of neutral and charged atoms has opened up a new and exciting region of physics that was previously inaccessible. Recent years have seen increasing use of optical trapping and cooling methods to create and control ultracold quantum gases, with trap depths in the microkelvin region. As experimental setups continue to advance, it is obvious that the ability to efficiently transport a cloud of cold atoms over macroscopic distances becomes crucial.

This particular experiment aims to interface ultracold atoms with nanomechanical devices - a hybridization that takes advantage of the cold atoms' ability to store quantum information, and the nanomechanical resonator's ability to communicate said information. The aim is accomplished by magnetically coupling the spin of the ultracold atoms with a time-dependent magnetic field - generated through a permanent magnetic film - on the nanomechanical resonator (See Figure 1). Given that the atoms are close enough to the resonator, and the energy difference between spin states matches that of the oscillating magnetic field, the motion of the oscillator is then coupled to the spin states of the ultracold atoms. This

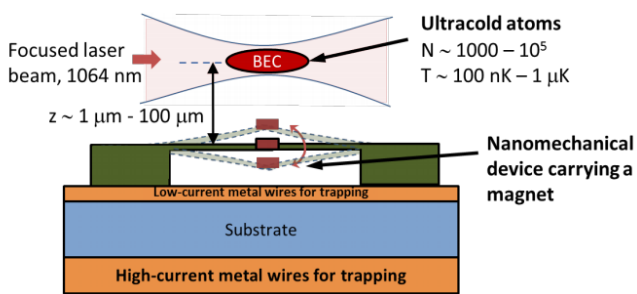


FIG. 1: Schematic of the atom-chip design for hybridizing a cloud of ultracold atoms with a nanomechanical resonator.(Credit: E. Saglamyurek, L. Leblanc.)

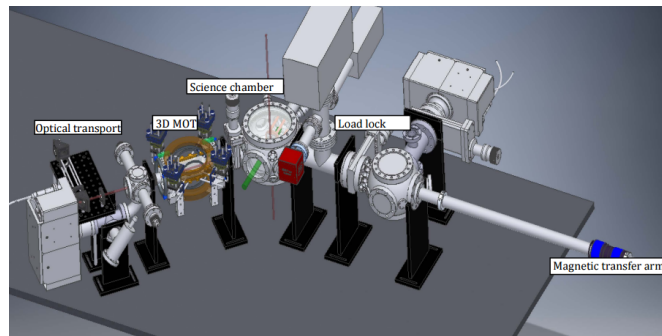


FIG. 2: Hybrid quantum system apparatus. ⁸⁷Rb atoms are cooled to microKelvin temperatures with a 3D MOT in the 3D MOT chamber. Atoms are then transferred using the optical transport system to the Science chamber where they are hybridized with nanodevices. The load lock and magnetic transfer arm are used to exchange nanodevices rapidly. (Credit: E. Saglamyurek, L. Leblanc.)

allows for transfer of information between the resonator and the atoms.^{[2],[3]}

Transport is a necessity for a few reasons, the simplest of which is spatial considerations: the hybridization site needs to interface with external systems, and the infrastructure required for cooling atoms are quite sizeable, which results in a conflict of space. Secondly, the state of the ultra high vacuum between the 3D MOT chamber and the Science chamber needs to be different (see Figure 2). Magneto-optical trapping works collects ⁸⁷Rb atoms as they wander into the trapping region, which necessarily includes an ambient background of freely moving atoms. This background cannot be present in the Science chamber, as it would interfere with the interaction between the nanomechanical device and the gas cloud. We remove this background by connecting the two chambers with a thin, long tube. Using optical transport, the atomic gas cloud can be directed to the science chamber. However, ambient rubidium atoms with a randomized velocity vectors are less likely to be able to make the journey.

Transport can be done in a variety of different ways, each with their advantages and drawbacks. Magnetic

*Electronic address: mengxing@ualberta.ca

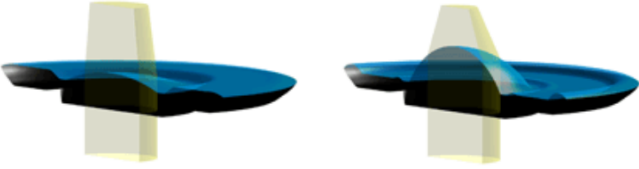


FIG. 3: Diagram of Optotune electrical lens EL-10-30. The lens shaper ring pushes down on the membrane, increasing pressure with current. This pumps liquid into the center of the lens and focuses the light. (www.optotune.com/technology/focus-tunable-lenses)

traps have been shown to be successful. However, their implementation involves moving coils or installing a chain of coils,^[4] which are spatially exhaustive and cumbersome in our set up. Optical lattices can be slightly detuned in order form a propagating standing wave.^[6] However, this technique is limited in its range due to its weak radial confinement, and is therefore incompatible with our experimental apparatus. Optical tweezers is a technique that gives a very tight trap, and the transport is achieved by mounting the focusing lens on a horizontal translation stage.^[5] However, it has the weakness of transferring mechanical vibrations from the movement of the stage to the atomic gas cloud. In order to eliminate this problem, we instead move the focus of the laser thorough the use of focus-tunable lenses. These lenses from the company *Optotune* feature optical fluids sealed inside a polymer membrane. A circular ring that pushes onto the center of the membrane is able to change the shape of the lens, and by extension, its focal length. The degree to which the focal length is changed is related to the current applied. Using these lenses eliminates the need for a translation stage, and the possibility of disrupting the quantum gas cloud with vibrations.^[1]

We outline three major pieces of theory required to achieve optical transport:

1. Creating an two dimensional optical trap using a red-detuned dipole trap.
2. Understanding the movement of the trap through gaussian beam propagation theory.
3. Optimizing non-adiabatic transport in order to minimize heating the atomic system and loss of atoms.

In step with understanding theory, we will also need to develop the physical system. The experimental aspects required are:

1. Building the optical set up for optical transport.
2. Developing LabView code to control focus tunable lenses from *Optotune*.
3. Measure actual rates of heating inside the trap.

To accomplish this, we make use of an 11W infrared laser with 1064nm wavelength. This is the laser that will be used to create the optical dipole trap for the cloud. To create the trap, the laser is sent through a series of three lenses. Two of these lenses are from the company Optotune, and their focal length can be tuned through the application of a current. Manipulating these focal lengths will be the basis of optical transport. Lastly, we make use of kinetic theory to model heating within the trap. The system will be controlled through a LabView program that we develop. Unfortunately, we do not currently have any rubidium atoms to trap, so we cannot make real measurements of heating.

II. TRAPPING

Red-detuned optical dipole trapping can be understood from the perspective of both classical and quantum mechanics. In classical mechanics, electrons on the atom can be modelled as a negative charge of mass m_e on the end of the spring. The laser light is an oscillating electric field \vec{E} of frequency ω , and so the system is merely a driven-damped-harmonic oscillator. The potential energy in this case is given by

$$U_{dip}(\vec{r}) = -\frac{1}{2}\langle\vec{p}\cdot\vec{E}\rangle = -\frac{1}{2\epsilon_0 c}Re(\alpha)I(\vec{r}) \quad (1)$$

where \vec{p} is the dipole moment, $I(\vec{r})$ is the intensity profile, and α is the atomic polarizability. The speed of light is c , and ϵ_0 is the permittivity of free space as usual. We can find α by solving the following.

$$-e\vec{x} = \vec{p} = \alpha\vec{E} \quad (2)$$

where \vec{x} is given by the equation of motion. The damping constant

$$\Gamma_\omega = e^2\omega^2/(6\pi\epsilon_0 m_e c^3) \quad (3)$$

is given by Larmor's formula for the radiative energy loss of an accelerated charge, ω_o is the natural resonance of the system, and $\vec{E}(t)$ denotes the time dependent driving electric field. From Newton's second law, we find

$$\ddot{\vec{x}} + \Gamma_\omega\dot{\vec{x}} + \omega_o^2\vec{x} = \frac{-e\vec{E}(t)}{m_e} \quad (4)$$

Solving this gives α as a function of Γ_ω . If we define the damping constant on resonance as $\Gamma = (\omega_o/\omega)^2\Gamma_\omega$, the the atomic polarizability is

$$\alpha = 6\pi\epsilon_0 c^3 \frac{\Gamma/\omega_o^2}{\omega_o^2 - \omega^2 - i(\omega^3/\omega_o^2)\Gamma} \quad (5)$$

$$Re(\alpha) = 6\pi\epsilon_0 c^3 \frac{\Gamma(1 - (\omega/\omega_o)^2)}{(\omega_o^2 - \omega^2)^2 + (\omega^3\Gamma/\omega_o)^2}$$

For red detuned traps, $\omega_o > \omega$, and $Re(\alpha) > 0$, so then $U_{dip} < 0$, and we have a trap. Physically, this means

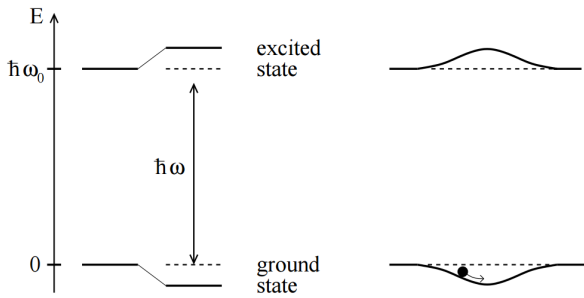


FIG. 4: Two-level atom model of optical dipole trapping. Left: Red detuned like shifts ground state energy down and excited state energy up, allowing a trap to be formed for atoms in the ground state. Right: Trap depth varies with light intensity. Trap produced from a laser beam with a gaussian intensity profile at the focus. (Figure from R.Grimm. 2000^[7])

that the atom is being driven in phase with the electric field, resulting in a lower energy configuration. Should the trap be blue detuned, then the electrons would be out of phase with the electric field, resulting in a higher energy configuration.

In semi-classical quantum mechanics, we assume a two level model and apply perturbation theory, as seen in Figure 4. Detuning is given by the difference between the driving frequency of the laser and the resonance frequency of the atom $\delta = \omega - \omega_0$. The resonance is defined for the ground to excited state transition, $\omega_0 = \omega_e - \omega_g$. Since the laser wavelength is so far detuned from atomic resonance, we can rightly ignore saturation effects. (That is, the excited level remains mostly empty, and most atoms remain in their ground state.) In doing so we can produce the same atomic polarizability, but Γ , rather than being the damping constant, is the spontaneous emission rate, and can be observed through the line width of the transition. For the ground state transition of ⁸⁷Rb, this value is given by the matrix element $|\langle \phi_e | \vec{r} | \phi_g \rangle|$, which is a measure of the wavefunction overlap of ground and excited states.

$$\Gamma = \frac{\omega_0^3}{3\pi\epsilon_0\hbar c^3} |\langle \phi_e | \vec{r} | \phi_g \rangle|^2 \quad (6)$$

$$= 2\pi(6.065\text{MHz})$$

Using this definition, the strength of the trap is then (with spatially depending intensity),

$$\Delta E(\vec{r}) = U(\vec{r}) = \frac{3\pi c^2 \Gamma}{2\omega_0^3 \delta} I(\vec{r}) \quad (7)$$

Before we move on, we must consider a competing mechanism, that is the scattering rate Γ_ρ . Although the light contributes no *net* momentum over time, it does still heat the system and has the potential to knock atoms out of a shallow trap. The scattering rate is given by

$$\Gamma_\rho = \frac{3\pi c^2}{2\hbar\omega_0^3} \frac{\Gamma^2}{\delta^2} I(\vec{r}) \quad (8)$$

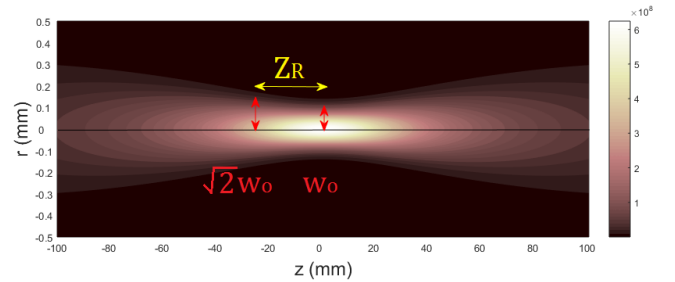


FIG. 5: Intensity profile of a laser going through a focus. The waist of the laser W is defined at the point where the intensity is $I(W) = I_0/e$. The Rayleigh length is defined as the distance between the two points where the $W = \sqrt{2}W_0$, where W_0 is the waist of the laser at the focus.

From Eq. 7 and Eq. 8, we see that for large detuning δ , the scattering rate decreases faster than the trap becomes shallow, so the trapping mechanism “wins out” over the heating, and in the steady state solution we have a cloud of trapped atoms.

From Eq. 7, we also see that the trap would be deepest at the point with the highest intensity: this is at the focus of the laser. In reality, laser beams do not focus to an infinitesimal point, instead the spot size of a laser at the focus is determined by a quantity called the waist. A picture definition of the waist and the Rayleigh range is shown in Figure 5. The waist in general can be related to the waist and the focus through the Rayleigh range, $z_R = \pi W_0^2 / \lambda$.

$$W(z) = W_0 \sqrt{1 + \frac{z^2}{z_R^2}} \quad (9)$$

Using these definitions, the shape of the trap is given by

$$U(\vec{r}, z) = \frac{3\pi c^2 \Gamma}{2\omega_0^3 \delta} \frac{2P}{\pi W(z)^2} e^{-\frac{2r^2}{W(z)^2}} \quad (10)$$

$$= U_0 e^{-\frac{2r^2}{W(z)^2}}$$

The model of this trap is shown in Figure 6 (left). It is important to note that the trapping in the radial direction is much tighter than trapping in the propagation direction z , and so the trap is in the shape of an oblong cigar. For small oscillations at low energies, the trap can be approximated as an anisotropic two dimensional harmonic oscillator (Figure 6 (right)).

$$U(\vec{r}, z) = U_0 - \frac{1}{2} m \omega_r^2 r^2 - \frac{1}{2} m \omega_z^2 z^2 \quad (11)$$

where $\omega_r = \sqrt{4U_0/mW_0^2}$, and $\omega_z = \sqrt{2U_0/mz_R^2}$. The trapping model for a 10W laser at a wavelength of 1064nm. From literature, we expect a waist of $W_0 = 50\mu m$ at the focus. ^[1] These parameters give $\omega_r = (2\pi)(1.13 \times 10^3 Hz)$ and $\omega_z = (2\pi)(5.40 Hz)$. The depth of the trap for the same parameters is $U_0/k_B = 328\mu K$.

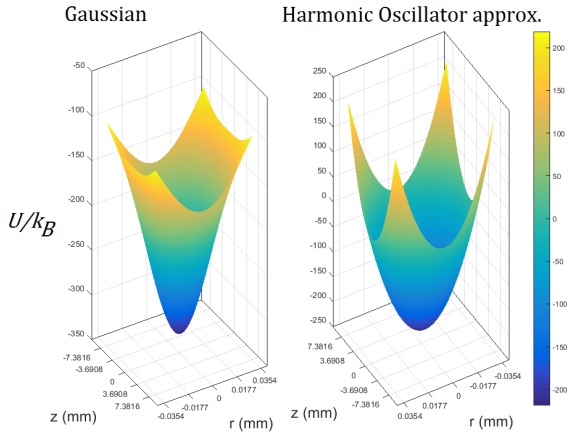


FIG. 6: Left: Optical trap for ^{87}Rb , with a resonant wavelength of 780.24nm . This model is based on specs of a 10W laser with wavelength 1064nm . Right: Harmonic oscillator approximation for the optical trap.

III. GAUSSIAN BEAM PROPAGATION

The intensity profile of the laser beam is not uniform across its intersection; the intensity is modulated and decreases steadily from the center to the edges. This is due to the diffraction of light as it propagates through free space. Most lasers adopt the gaussian intensity profile, which is its fundamental mode (TEM00). This mode is particularly important as it gives tightest focus when the beam is passed through a lens.

The setup aims to move the trap at a constant waist, and this has been done before.^[1] Following the general schematic of the set up from Leonard *et al.* (Figure 7), we double check the calculations with ABCD beam propagation matrices.

We begin with a collimated beam, defined by the complex beam parameter q_i as determined by the input waist

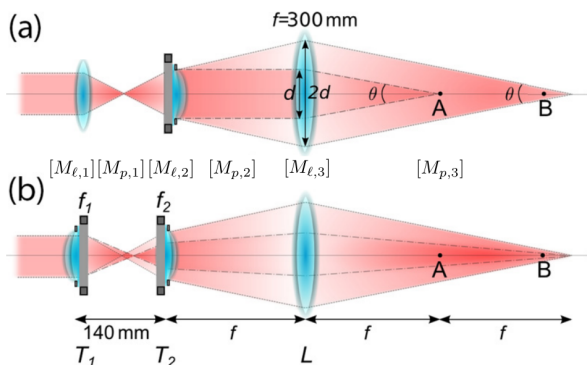


FIG. 7: Set up of optical transport using 2 tunable focus lenses. Top: Transport and constant waist using one focus tunable lens. Bottom: Transport with independent control over the waist and position using two focus tunable lenses. Figure from Leonard *et al.*, 2014.

and the frequency (in the Rayleigh range), as well as the radius of curvature of the beam wavefronts R :

$$\frac{1}{q_i} = \frac{1}{R_i} - \frac{i}{z_{Ri}} \quad (12)$$

Since the input beam is collimated, $R = \infty$, so the complex beam parameter is purely imaginary. Our ABCD matrix, $[M_{sys}]$ is computed from multiplying lens matrices and free space propagation matrices, according to the order in which our beam encounters them.

$$\begin{aligned} \text{Thin lens matrix:} &= [M_{\ell,i}] = \begin{pmatrix} 1 & 0 \\ -\frac{1}{f_i} & 1 \end{pmatrix} \\ \text{Free space:} &= [M_{p,i}] = \begin{pmatrix} 1 & d_i \\ 0 & 1 \end{pmatrix} \\ \text{System matrix:} &= [M_{sys}] = \begin{pmatrix} A & B \\ C & D \end{pmatrix} \end{aligned} \quad (13)$$

In our system,

$$[M_{sys}] = [M_{p,3}][M_{\ell,3}][M_{p,2}][M_{\ell,2}][M_{p,1}][M_{\ell,1}] \quad (14)$$

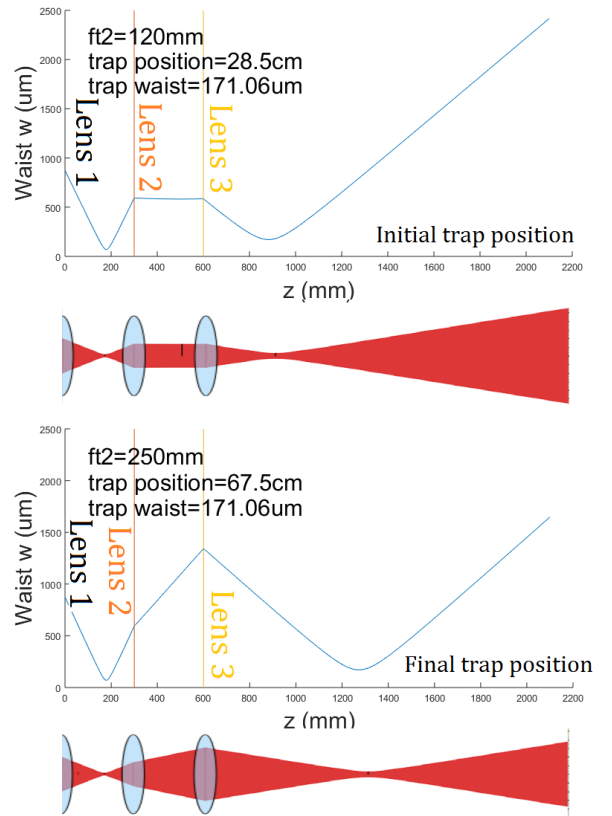


FIG. 8: Top: Initial trap position, with the focus-tunable lens (middle lens) set at a focal length of 100mm . Bottom: Final trap position, with the focus-tunable lens set at a focal length of 250mm . The other two lenses are fixed, with focal lengths of 180mm (left) and 300mm (right). Note that the waist is constant.

The outgoing beam is then defined by

$$\frac{1}{q_f} = \frac{C + D/q_i}{A + B/q_i} = \frac{1}{R_f} - \frac{i}{z_{Rf}} \quad (15)$$

Where we can extract the beam waist from the Rayleigh range in the imaginary component. By varying the distance propagated, we can trace out the waist at each step. One possible arrangement is shown in Figure 8, using numbers that come from characterization of the laser beam and the Optotune lenses. The size of the waist at the focus is linearly related to the input waist size by,

$$W_o = \frac{f\lambda}{\pi W_{in}} \quad (16)$$

We can use this property to characterize the transport of the system. In addition, the waist at the focus is inversely proportional to the input waist – which makes sense, the more spatial frequencies input into the system, the better the position of the focus will be defined. Therefore, having a large input beam size will give a tighter trap.

In the model given by Figure 8, we used input parameters measured from the laser and specifications of the Optotune lenses. The input waist size is $W = 1748\mu\text{m}$, lens 1 was held at $I = 290\text{mA}$, which corresponds to a focal length of $f_1 = 180\text{mm}$. Lens 2 was tuned with focal lengths $120\text{mm} - 250\text{mm}$, and lens 3 is fixed, with a focal length of 300mm . Output parameters shows a total transport of 39cm at a waist of $171.06\mu\text{m}$. 39cm is more transport distance than we need, which is great, but the waist size is larger than we'd like, which would compromise the trap depth we had originally envisioned. The waist size is not close to the aperture of the lenses at any point, so we do not expect any clipping.

IV. NON-ADIABATIC TRANSPORT

In order to transport the atoms without “spilling” them from the trap, we study the heating of atoms induced by movement of the trap. In order to move the atoms adiabatically, we need to transport them over a time duration that is much larger than their natural oscillation period. Since transport is done along the z axis, we will focus the harmonic trap in the z dimension. Previously, we modelled the natural oscillation frequency of the trap along z to be $\omega_z = 33.9\frac{\text{rad}}{\text{s}}$. This gives an oscillation period of $T = 2\pi/\omega_z = 0.185\text{s}$. To ensure the adiabatic regime, we need a duration approximately a thousand times that of the natural oscillation period, which gives 185s , just a little more than 3 minutes. Measurements of quantum gas clouds in cold atom experiments are done using destructive absorption or fluorescence imaging, so the sample needs to be prepared many times for a single data set. Three minutes is longer than we would like to wait in the experiment for the transportation of atoms, given the necessary high repetition

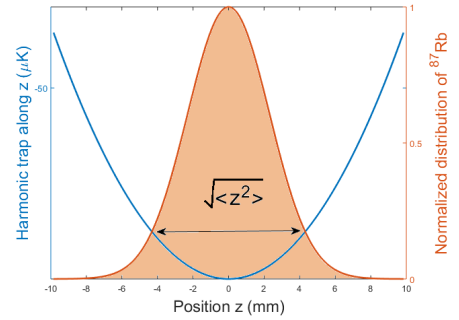


FIG. 9: Normalized distribution of thermalized distinguishable particles in an harmonic trap.

rate, so we do not have the luxury of using the adiabatic regime.

More importantly, the population of atoms inside the trap are given by

$$N = N_o e^{-t/\tau} \quad (17)$$

The atoms in the trap are continually being lost to the surroundings due to background collisions, and possess an average life time of $\tau \simeq 60\text{s}$ before being kicked out of the trap. Therefore, in order to maintain a large population of atoms with which to experiment, transport time must be shortened.

We begin with a simple model by assuming the particles in the trap are distinguishable thermal particles governed by the Boltzmann distribution. In this regime, the number of particles is given by

$$N = \frac{1}{h^3} \int d^3\vec{p} d^3\vec{r} e^{-\vec{H}(\vec{r},\vec{p})/k_B T} \quad (18)$$

For our system, the Hamiltonian is a harmonic oscillator with $m = m_{Rb}$,

$$\vec{H} = \frac{p^2}{2m} + \frac{1}{2}m\omega_z^2 z^2 + \frac{1}{2}m\omega_r^2(x^2 + y^2) \quad (19)$$

which gives a total number of particles given by

$$N = \left(\frac{k_B T}{h}\right)^3 \frac{1}{\omega_z \omega_r^2} \quad (20)$$

Then the density of particles in position space is simply the integral over momentum. For a harmonic oscillator potential, this distribution has the shape of a gaussian, as seen in Figure 9 and Equation 21.

$$n(\vec{r}) = \left(\frac{mk_B T}{2\pi\hbar^2}\right)^{\frac{3}{2}} e^{-\frac{m(\omega_z^2 z^2 + \omega_r^2(x^2 + y^2))}{2k_B T}} \quad (21)$$

The average value of position $\langle r \rangle$ is zero in a symmetric potential like this, so we relate thermodynamic quantities

to $\langle r^2 \rangle$. We add the normalization factor N to get

$$\begin{aligned} \langle r^2 \rangle &= \frac{1}{N} \int_{-\infty}^{\infty} (x^2 + y^2 + z^2) e^{-\frac{m(\omega_z^2 z^2 + \omega_r^2(x^2 + y^2))}{2k_B T}} dx dy dz \\ &= \frac{k_B T}{m} \left(\frac{1}{\omega_z^2} + \frac{2}{\omega_r^2} \right) \end{aligned} \quad (22)$$

The value $\langle r^2 \rangle$ is measured from the oscillation amplitude of the distribution in the trap after transport. Since we are only transporting in one dimension, and the internal collisions of the particles do not change the overall energy of the system. Therefore, we can just measure the oscillation amplitude of the center of mass. Furthermore, if we are only looking for the *change* in temperature, we only need to look at $\Delta \langle z^2 \rangle$.

$$\begin{aligned} \langle \Delta z^2 \rangle &= \frac{k_B \Delta T}{m \omega_z^2} \\ \Delta T &= \frac{m \omega_z^2 \langle z^2 \rangle}{k_B} \end{aligned} \quad (23)$$

To do this, we need to study the force exerted on the atoms from the movement of the trap, and solve the subsequent equation of motion for $\vec{z}(t)$. The movement of the trap can be viewed as a fictitious force applied on the atoms in the non-inertial reference frame that moves with the center of the trap. Then by Newton's second law, the equation of motion is

$$\begin{aligned} m \ddot{z}(t) &= m \ddot{z}_c(t) - m \omega_z^2 z(t) \\ \ddot{z}(t) + \omega_z^2 z(t) &= \ddot{z}_c(t) \end{aligned} \quad (24)$$

where $\ddot{z}_c(t)$ is the acceleration profile of the trap, and $z(t)$ is the motion of particles within the trap in the frame moving with the centre of trapping potential. This is an inhomogeneous 2nd order differential equation with homogeneous solutions

$$z(t) = A \cos(\omega_z t) + B \sin(\omega_z t) \quad (25)$$

Using the boundary conditions $x(0) = 0$, we stick with the solution involving sines and write it in terms of exponentials, which gives

$$z(t) = \frac{B}{2i} (e^{i\omega_z t} - e^{-i\omega_z t}) \quad (26)$$

We then solve the inhomogeneous equation by using the method of variation of parameters. Hypothesizing the particular solution

$$z_p(t) = \frac{B}{2i} (u_1(t) e^{i\omega_z t} - u_2(t) e^{-i\omega_z t}) \quad (27)$$

Plugging this solution back into Eq. 24 gives

$$\begin{aligned} u_1(t) &= \frac{1}{B \omega_z} \int_0^t \ddot{z}_c(t') e^{-i\omega_z t'} dt' + c_1 \\ u_2(t) &= \frac{1}{B \omega_z} \int_0^t \ddot{z}_c(t') e^{i\omega_z t'} dt' + c_2 \end{aligned} \quad (28)$$

The particular solution is then (absorbing B into the definition of u_1 and u_2),

$$z_p(t) = \frac{1}{\omega_z} \int_0^t \ddot{z}_c(t') \sin(\omega_z(t-t')) dt' \quad (29)$$

Up until this time we have assumed that the acceleration profile is defined for some duration $0 \leq t \leq t_f$, and zero otherwise. In order to proceed, we must make some further assumptions.

1. The acceleration profile is antisymmetric, or odd.
 - (a) Taking advantage of this, we perform a time domain shift from $0 \leq t \leq t_f \rightarrow -\frac{t_f}{2} \leq t \leq \frac{t_f}{2}$.
2. The initial and final velocities of the trap are zero. ($\dot{z}_c(-\frac{t_f}{2}) = \dot{z}_c(\frac{t_f}{2}) = 0$)

Under these assumptions, the particular solution can be written as

$$\begin{aligned} z_p(t) &= \frac{1}{\omega_z} \int_{-\frac{t_f}{2}}^{\frac{t_f}{2}} \ddot{z}_c(t') \sin(\omega_z(t-t')) dt' \\ &= \int_{-\frac{t_f}{2}}^{\frac{t_f}{2}} \dot{z}_c(t') \cos(\omega_z(t-t')) dt' \end{aligned} \quad (30)$$

Where we use integration by parts and boundary conditions to set the boundary term to zero. Next we expand cosine and factor out the t dependence in the exponentials, which gives

$$\begin{aligned} z_p(t) &= \frac{1}{2} \left(e^{i\omega_z t} \int_{-\frac{t_f}{2}}^{\frac{t_f}{2}} \dot{z}_c(t') e^{-i\omega_z t'} dt' \right. \\ &\quad \left. + e^{-i\omega_z t} \int_{-\frac{t_f}{2}}^{\frac{t_f}{2}} \dot{z}_c(t') e^{i\omega_z t'} dt' \right) \end{aligned} \quad (31)$$

Since $\ddot{z}_p(t)$ is antisymmetric, $\dot{z}_p(t)$ is symmetric, so the two integrals are actually identical and can be factored out. Which gives the particular solution

$$\begin{aligned} z_p(t) &= \frac{1}{2} (e^{i\omega_z t} + e^{-i\omega_z t}) \int_{-\frac{t_f}{2}}^{\frac{t_f}{2}} \dot{z}_c(t') e^{-i\omega_z t'} dt' \\ &= \cos(\omega_z t) \mathcal{F}[\dot{z}_c(t)] \end{aligned} \quad (32)$$

The oscillatory part of the motion is given by $\cos(\omega_z t)$, and the amplitude is given by the integral, which we recognize as the Fourier transform of the velocity profile at ω_z . To model the temperature of atoms inside the trap then, we need to specify a trap profile that satisfies our assumptions. Following previous work by Couvert *et al.*, we decide to model the position profile of the trap using an error function, see Figure 10. The position, velocity,

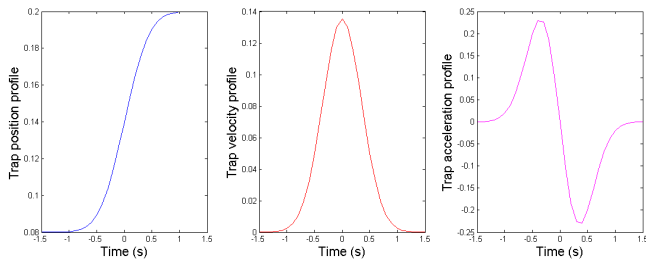


FIG. 10: Transportation profile of the trap. Left: Position profile defined by the error function. Middle: Velocity profile in the shape of a gaussian. Right: Antisymmetric acceleration profile.

and acceleration profiles of the trap are as follows:

$$\begin{aligned} z_c(t) &= \frac{|F_f - F_i|}{2} \left[\operatorname{erf}\left(\frac{6t}{t_f}\right) + 1 \right] + F_i \\ \dot{z}_c(t) &= \frac{6}{\sqrt{\pi}} \frac{|F_f - F_i|}{t_f} e^{-9\left(\frac{2t}{t_f}\right)^2} \\ \ddot{z}_c(t) &= \frac{6}{\sqrt{\pi}} \frac{|F_f - F_i|}{t_f} e^{-9\left(\frac{2t}{t_f}\right)^2} \left(-\frac{72t}{t_f^2} \right) \end{aligned} \quad (33)$$

where F_i and F_f are the initial and final positions of the trap. The Fourier transform of this velocity profile is given by

$$A = |F_f - F_i| e^{-\frac{(\omega_z t_f)^2}{12}} \quad (34)$$

The temperature change of the system is then

$$\Delta T = \frac{m\omega_z^2 A^2}{2k_B} \quad (35)$$

As a function of t_f , both the temperature and oscillation amplitude is a gaussian, as shown in Figure 11. As we can see for short wait times of $t_f \leq 0.6s$, the atoms will easily be spilt from the trap. However, the temperature increase decreases dramatically as a function of wait time thanks to the suppression of the exponential term. Zooming in on the area of interest, we see that for durations longer than $0.6s$, we are well below the approximate trap depth.

V. SET UP CHARACTERIZATION

The following section goes through some basic characterization of the setup, beginning with the spot size. As mentioned earlier, a larger incoming beam (larger waist) will result in a tighter trap. The spot size of the laser is shown in Figure 12. It can be seen that the spot is slightly elliptical in shape, with slight amounts of clipping in the x-axis. This will likely be remedied with more careful alignment. Nevertheless, we calculate the average waist to be

$$W_{\text{ave}} = \frac{1}{2}(W_x + W_y) = 1748\mu m \quad (36)$$

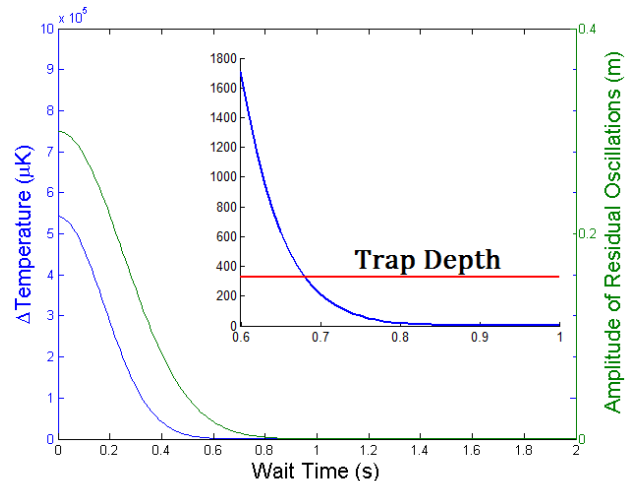


FIG. 11: Temperature of atoms in the trap, with δt set close to the natural resonance of the trap. Inset: Temperature and amplitude profile at $0.6 \leq t_f \leq 1$. The green line is the approximate trap depth.

Which gives a waist-at-focus of

$$W_o = 171\mu m \quad (37)$$

This is close to the $50\mu m$ that we assumed for our models, and exceeds our expectations, which would make our model even better.

The transport system is composed of two focus tunable lenses from Optotune and one fixed focus lens. Of the tunable focus lenses, TF1 has a long focal range and will be used to adjust waist. In the tightest configuration, we keep TF1 at a focal length of approximately $18.2cm$, at a current of $290mA$. The characterization of TF1 is shown in Figure 13. This function is best fitted by a quadratic

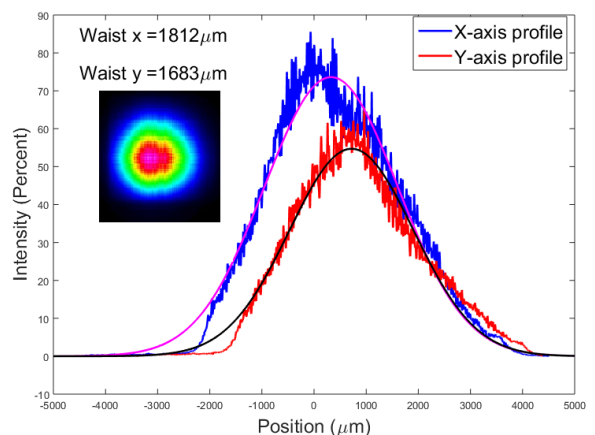


FIG. 12: Spot characterization of the $1064nm$ laser. Here the laser power is held at $0.1W$. Inset: Picture of the spot as taken by the Thorlabs beam profiler.

function, which is given by

$$F = 0.0016 \frac{\text{cm}}{\text{mA}^2} I^2 - 0.9115 \frac{\text{cm}}{\text{mA}} I + 152.65 \text{cm} \quad (38)$$

The waist as a function of the focus can be fitted with Equation 16, which gives an input waist of $1350 \pm 40 \mu\text{m}$. Similarly, the current-to-focus relationship for TF2 is shown in Figure 14. Its relationship is fitted by a quadratic equation. (Although the Optotune manual shows a linear relationship between current and focus, we found a quadratic to give a better fit.)

$$F = 0.0002 \frac{\text{cm}}{\text{mA}^2} I^2 - 0.109 \frac{\text{cm}}{\text{mA}} I + 24.6 \text{cm} \quad (39)$$

Again the input waist is fitted to be $1610 \pm 50 \mu\text{m}$. Averaging the two fitted waists and comparing them to the measured waist, we find a percent difference of

$$\begin{aligned} \% \text{Difference} &= \frac{|\text{Expected} - \text{Measured}|}{\text{Expected}} \times 100 \\ &= \frac{|1748 \mu\text{m} - 1540 \mu\text{m}|}{1748 \mu\text{m}} \times 100 = 11.9\% \end{aligned} \quad (40)$$

We attribute this difference of waists to the slight divergence of the laser beam, which would result in a different spot size and waist measurement between the point where the spot profile was taken, and the point where it passes through the lens.

Having characterized each of the lenses, we construct the system and look at the combined change in trap position as a function of current applied to TF2. Here we

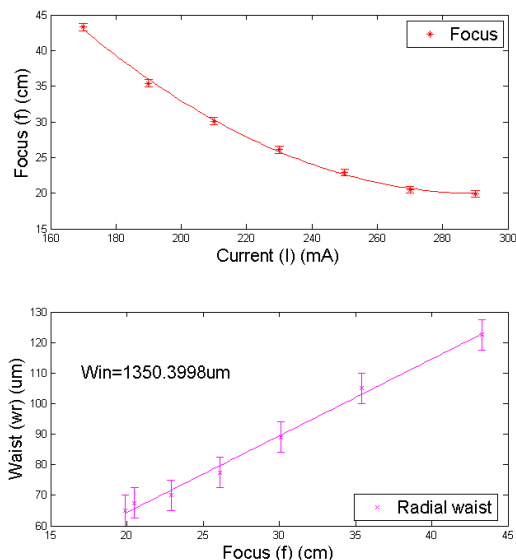


FIG. 13: Focus as a function of current applied for the first tunable focus lens, TF1. The waist at the focus is calculated and fitted to check the input waist.

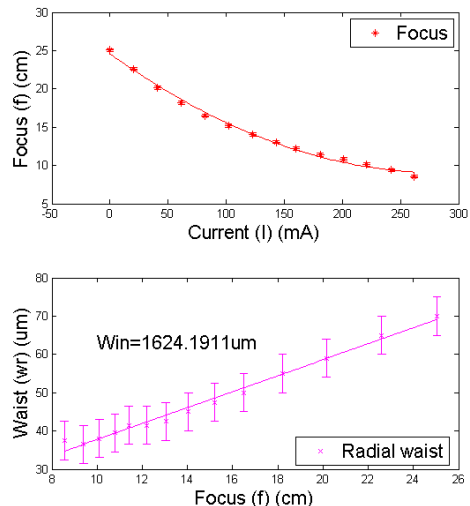


FIG. 14: Focus as a function of current applied for the second tunable focus lens, TF2. The waist at the focus is calculated and fitted to check the input waist.

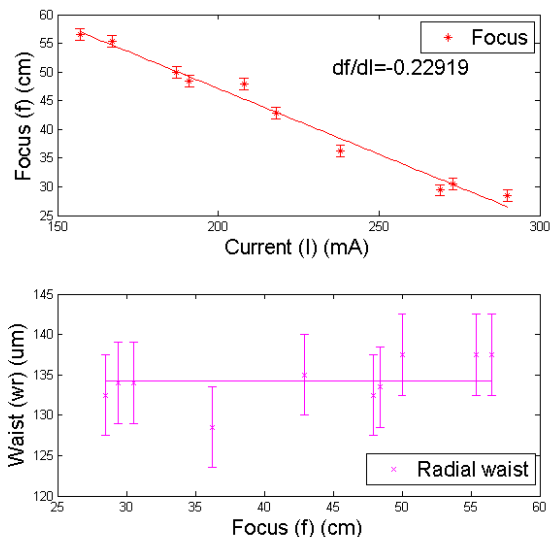


FIG. 15: Focus as a function of current applied to the second tunable focus lens, for the transport system of three lenses. TF1 is held at a current of 290mA . The current for TF2 is manipulated to change the position of the waist. The size of the waist is predicted to be constant.

keep TF1 at 290mA , which corresponds approximately to a focal length of $(18.2 \pm 0.5) \text{cm}$. Lens 3 is fixed with a focal length of 30cm . Surprisingly, unlike the characterization of single lenses, the focus of the transport system corresponds linearly to current, as can be seen in the top graph of Figure 15. The equation describing this is given

by

$$F_{\text{sys}} = -0.23 \frac{\text{cm}}{\text{mA}} I + 92.95 \text{cm} \quad (41)$$

The waist of the system is predicted to be constant, and we can see in the bottom graph of Figure 15 that this is true within error. The waist is measured to be

$$W_o = (135 \pm 5) \mu\text{m} \quad (42)$$

As the focal lengths are long in these measurements, the accompanying error is large. However, our system operates within parameters necessary for the transportation of atoms, and is actually better than the modelled $171 \mu\text{m}$. Nevertheless, a waist of $135 \mu\text{m}$ gives a trap depth of $30 \mu\text{K}$ (laser power dependent), and we would ideally like a trap depth of at least $50 \mu\text{K}$. Our computational model shows that using a shortening the focal length of lens 1 from 18cm to 10cm will accomplish give a waist of $115 \mu\text{m}$, which gives a trap depth of $62 \mu\text{K}$.

There is yet another complication. Despite our efforts, the transport will never be infinitely smooth. Time steps and current settings are discrete, so the velocity profile is not a perfect gaussian. The limit of the step sizes are limited by the communication time between the lens controller and the lens, our rudimentary Labview code sets this at 100ms currently, but obviously the shorter we make this, the smoother transport will be.

In order to account for the finite step size, we make use of Matlab's numerical FFT function to compute the Fourier transform of a non-smooth function. The results are shown in Figure 16. For time step $dt = 80 \text{ms}$, the velocity profile is quite jagged, and gets smoother as the total duration increases. We can see that the temperature profile of the jagged velocity profile is indeed higher than the infinitely smooth analytical solution; however, we are still able to keep well within the limits of the trap, so there is no significant cause for concern.

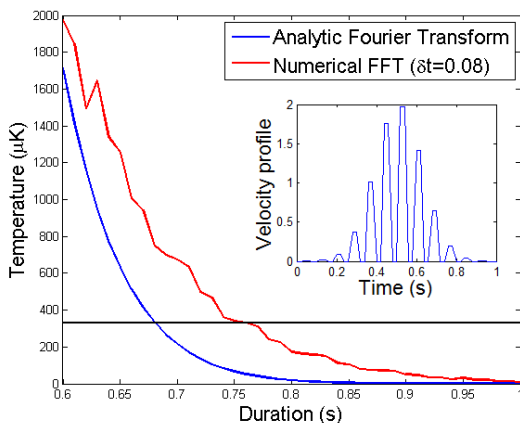


FIG. 16: Numerical FFT amplitude versus the infinitely smooth analytical solution. The two are similar enough to not be cause for significant concern. Inset: Velocity profile used in the numerical FFT.

VI. FUTURE WORK

This project has been a small but instrumental piece of the larger hybridization project. As of now there are still a few pieces remaining before transport is possible.

LabView code has been developed to control the lenses TF1 and TF2 separately. In order to facilitate timing of the current change, it would be best if both lenses were controlled from the same LabView VI. In addition, the current LabView code has a communication time cap of approximately 500ms , which is a little too long of a time step. (Model computed using 80ms time steps in Figure 16). Ideally this would be as short as possible for smooth transport. Heating of the system also needs to be characterized, once the atoms come in.

VII. CONCLUSION

For this 499 project, I undertook the task to transfer ultracold atoms a distance of approximately 30cm from the 3D MOT chamber to the hybridization science chamber. This transport is to be a part of the experiment that couples ultracold atomic clouds to nanomechanical devices in order to study quantum information storage and communication.

To do this, an optical dipole red-detuned trap was created using a 10W infrared laser with 1064nm . This type of trap is well known and can be understood using both classical mechanics of a damped driven oscillator as well as the semi-classical model of a two-level atom.

Translation of the trap, which is located at the focus of the laser, is done using focus tunable lenses from Optotune. This idea is based on a paper by Leonard et al., and has advantages of spatial efficiency and vibration isolation over some other techniques that exist. We successfully modeled the movement of the trap using gaussian beam propagation matrices and created the setup using a cage system from Thorlabs. Preliminary LabView code was developed for controlling the lenses, but could be improved upon.

We used kinetic theory to determine the change temperature of atoms as the trap propagates. We found that in order to minimize heating, the amplitude of residual oscillations (oscillations of the cloud after transport) must be small. This amplitude is the Fourier transform of the velocity profile. For a gaussian velocity profile (position modeled by an error function), heating inside the trap could be reduced to a manageable level.

Lastly, we designed the set up and characterized the system. This includes current to focus relationships for TF1 and TF2, as well as spot size measurements and waist-at-focus measurements. A summary of results is shown below.

Spot size:

$$W_{in} = (1540 \pm 50) \mu\text{m} \quad (43)$$

TF1 Current-to-focus equation:

$$F = 0.0016 \frac{\text{cm}}{\text{mA}^2} I^2 - 0.9115 \frac{\text{cm}}{\text{mA}} I + 152.65 \text{cm} \quad (44)$$

TF2 Current-to-focus equation:

$$F = 0.0002 \frac{\text{cm}}{\text{mA}^2} I^2 - 0.109 \frac{\text{cm}}{\text{mA}} I + 24.6 \text{cm} \quad (45)$$

System Current-to-focus equation:

$$F_{\text{sys}} = -0.23 \frac{\text{cm}}{\text{mA}} I + 92.95 \text{cm} \quad (46)$$

Waist at focus:

$$W_o = (135 \pm 5) \mu\text{m} \quad (47)$$

VIII. ACKNOWLEDGEMENTS

Overall, this was a great project - I learned many skills, encompassing theory, computational modelling, and experimental techniques. It opened my eyes to the kind of work that is currently being done in the field, and I am very excited for what is to come. I would like to thank Dr. Lindsay Leblanc for the opportunity to work in her lab, and for all the assistance she provided along the way.

-
- [1] J. Leonard, M. Lee, A. Morales, T. Karg, T. Esslinger, and T. Donner. (2014). *New Journal of Physics*, **16**, 093028.
- [2] Y. Wang, M. Eardley, S.Knappe, J. Moreland, L. Hollberg, J. Kitching. (2006). *Phys. Rev. Lett.*, **97**(227602)
- [3] C. Montoya, J. Valencia, A. Geraci. (2015). *Phys. Rev. A*, **91**(063835)
- [4] M. Greiner, I. Bloch, T. W. Hänsch, T. Esslinger. (2001). *Phys. Rev. A*, **63**(031401(R))
- [5] T. L. Gustavson, A. P. Chikkatur, A. E. Leanhardt, A. Görlitz, S. Gupta, D.E. Pritchard, W. Ketterle. (2002). *88*(2)020401-(1-4)
- [6] S. Schmid, G. Thalhammer, K. Winkler, F. Lang, J. H. Denschlag. (2006). *New Journal of Physics*, **8**(159), DOI:10.1088/1367-2630/8/8/159
- [7] R. Grimm, M. Weidemuller, and Y. Ovchinnikov. (2000). *Advances in Atomic, Molecular, and Optical Physics* **42**, 95-170.
- [8] A. Couvert, T. Kawalec, G. Reinaudi, and D. Guery-Odelin. (2008). *Euro. Phys. Lett.* **83**, 13001.